Electromechanical Limits of Polymersomes

H. Aranda-Espinoza,[1] H. Bermudez,[2] F. S. Bates,[3] and D. E. Discher[1,2]

[1]*Institute for Medicine and Engineering, University of Pennsylvania, Philadelphia, Pennsylvania 19104*
[2]*School of Engineering and Applied Science, University of Pennsylvania, Philadelphia, Pennsylvania 19104*
[3]*Department of Chemical Engineering and Materials Science, University of Minnesota, Minneapolis, Minnesota 55455*

(Received 24 May 2001; published 24 October 2001)

Self-assembled membranes of amphiphilic diblock copolymers enable comparisons of cohesiveness with lipid membranes over the range of hydrophobic thicknesses $d = 3-15$ nm. At zero mechanical tension the breakdown potential V_c for polymersomes with $d = 15$ nm is 9 V, compared to 1 V for liposomes with $d = 3$ nm. Nonetheless, electromechanical stresses at breakdown universally exhibit a V_c^2 dependence, and membrane capacitance shows the expected strong d dependence, conforming to simple thermodynamic models. The viscous nature of the diblock membranes is apparent in the protracted postporation dynamics.

DOI: 10.1103/PhysRevLett.87.208301 PACS numbers: 82.70.Uv, 68.65.–k, 87.68.+z

A primary task for any biological membrane is to separate inside from out, partitioning ions and other solutes that generate a transmembrane potential V_m. Electrically excitable cells, particularly neurons, control and propagate this potential for purposes of signaling and intercommunication [1]. Efforts to exploit and better understand such phenomena have most recently motivated the semipatterned growth of nerve cells on circuits [2] as well as the generation of artificial networks with soft nanotubes pulled from vesicles [3]. Further opportunities in such directions now seem possible with wholly synthetic block copolymers that, analogous to lipids in water, self-assemble into membranes, minimizing interfacial exposure of hydrophobic segments (Fig. 1) and thereby generating vesicles termed polymersomes [4].

Physical limits of self-assembled lipid membranes impose important constraints on electrochemical signals. Indeed, the operating range of biomembrane excitations, such as the action potential of a neuron, is generally less than 0.1 V over time scales of milliseconds. At the same time, a finite resting tension τ is exerted on most cell membranes, including neurons [5], through substrate adhesion and additional cellular mechanisms. Several experimental techniques have shown that τ is in the range of $0.01-0.1$ pN/nm [6], though additional transient stresses on cells can readily magnify such tensions [7]. For example, electrocompressive stresses arise with a voltage drop across a membrane and have long been recognized as being coupled to lateral tensions through an integrated form of the Lippmann equation [8]:

$$\tau + \tfrac{1}{2} C_m V_m^2 = \tau_{\text{net}}, \qquad (1)$$

where C_m is the capacitance per unit area of the membrane, and τ_{net} is an equivalent tension. The effects of the electrocompressive stresses have important implications when they are large enough to disrupt the membrane, a phenomenon known as electroporation [9]. When the disruption of the membrane is reversible, this technique can be used to load foreign macromolecules into cells [10] and to create hybrid cells [9]. The understanding of electroporation is an ongoing effort both theoretically and experimentally [10,11]. While cells are more structurally and compositionally complex than lipid membranes, there is a remarkable degree of qualitative agreement in the electromechanical behavior [9,12]. Thus, lipid membranes provide a simple model for the understanding of electroporation. Direct tests of lipid membrane cohesion by Needham and Hochmuth [13] have clearly demonstrated the electromechanical limits of lipid membranes via the combination of micropipette aspiration and electroporation techniques. From these and related tests it has become clear that transmembrane potentials higher than 1 V and mechanical tensions higher than ~10 pN/nm are not sustainable in lipid membranes [5,13]. Clearly, a hydrophobic thickness of only $d = 3-4$ nm for such membranes is a determinant of electromechanical stability.

Formation of polymersomes in dilute aqueous solutions has been described elsewhere [4]. Generally, the phase behavior of amphiphiles composed of strongly segregating segments is determined by the hydrophilic fraction f and mean molecular weight $\bar{M}_n$ [14]. Lipids provide initial guidance in the synthesis [15] of biomimetic

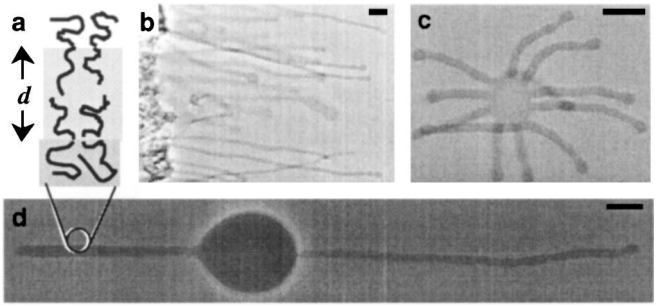

FIG. 1. (a) Polymersome membrane schematic. (b) Vesicular tubes sprouting out from bulk OB18 copolymer. (c), (d) OE7 vesicles exhibiting tubelike arms. Vesicles are observed using phase contrast with isotonic solutions of sucrose (inside) and glucose (outside). Scale bars are 10 μm.

TABLE I. Vesicle-forming amphiphiles: comparisons between lipids, SOPC and dimyristoyl-phosphatidylcholine (DMPC) [18], and diblock copolymers including d and f of the formed membranes. Cryo-TEM was used to estimate d for the polymersomes [4,17].

Molecule	Average structure	f	$\bar{M}_n$ (kDa)	$\bar{M}_w/\bar{M}_n$	d (nm)
DMPC	⋯	0.36	0.68	1	2.5 ± 0.06
SOPC	⋯	0.31	0.79	1	3.0 ± 0.06
OE7	$EO_{40} - EE_{37}$	0.39	3.9	1.10	8.0 ± 1.0
OB16	$EO_{51} - BD_{55}$	0.37	5.2	1.10	10.6 ± 1.0
OB18	$EO_{51} - BD_{126}$	0.29	10.4	1.10	14.8 ± 1.0

superamphiphiles. Table I shows $f \approx 29\%-39\%$ for vesicle-forming phospholipids and diblock copolymers, although the latter are much higher in $\bar{M}_n$ and somewhat more polydisperse. For the copolymers used here, the hydrophilic segment of polyethyleneoxide (PEO) forms a highly hydrated brush [16] while aggregation is driven by a hydrophobic block of either polyethylethylene (PEE) or its unsaturated homologue polybutadiene (PBD). As will be reported elsewhere [17], scaling of d with $\bar{M}_n$ (as well as elastic properties) is consistent with the hydrophobic core behaving as a fluidlike melt.

When small pieces of our copolymers are added to water, vesicular tubes spontaneously sprout and grow [Fig. 1(b)]. Vesicle formation processes — kinetics, yields, and morphologies — exhibit temperature dependences that likely stem from hydration-facilitated melting of PEO [15]. The formed vesicles exhibit a wide variety of shapes that range from multiarmed stars to hundreds of micron-long axonlike tubes (Fig. 1) as well as flaccid spheroids. Transformations between morphologies are easy to achieve through osmotic adjustments of the external solution [4] and thus reveal the semipermeable nature of the copolymer membranes. Our first generation polymersomes composed of a PEO-PEE diblock copolymer (designated OE7 in Table I) possess a core thickness $d \approx 8 \pm 1$ nm and have already been shown to be mechanically tough [4]. In this Letter, we elaborate on the more general electromechanical responses of polymersomes including two new covalently cross-linkable PEO-PBD copolymers of similar block fraction but higher molecular weight (OB16 and OB18 in Table I). Specific comparisons are made with our own measurements of the highly representative lipid stearoyl-oleoyl-phosphatidylcholine (SOPC), which are comparable to the results reported elsewhere [13,18]. Thus, for the first time we can thoroughly study the cohesiveness of membranes as a function of their hydrophobic core thickness over the range 3–15 nm.

Flaccid polymersomes were progressively aspirated into a micropipette (Fig. 2 inset) at stress rates of ~ 0.1 pN nm^{-1} sec^{-1} up to the point of rupture. Values of the lysis tension τ_c for SOPC as well as the three polymersomes studied are shown in Table II. The results generally show that increasing $\bar{M}_n$ leads to an increase in stability, consistent with general ideas of mesophase stability for strongly segregated copolymers [14]. As such, the hydrophobic core is expected to behave as a dense fluid. Assuming incompressibility, the thickness at rupture is given by $d_c = d/(1 + \alpha_c)$, where α_c is the area strain at rupture as measured directly from images of aspirated vesicles. For lipids, α_c is very small, typically 0.03–0.05 [18], so that $d_c \approx d$. For polymersomes, however, α_c ranges from 0.2 ± 0.06 for OE7 to 0.44 ± 0.06 for OB18. Thus, polymersomes should thin considerably. A simple linear fit of τ_c vs d_c is found to intersect the y axis at essentially zero tension (Fig. 2). Moreover, the slope of this fit defines a lysis stress $\Sigma_c = \tau_c/d_c \approx 27$ atm. Such a stress is typical of cavitation pressures for homogeneous fluids [19] suggesting that lysis of membranes can occur through nucleation of water-filled cavities inside the hydrophobic core.

Electromechanical experiments were performed to determine the breakdown potential V_c at different membrane tensions. Once again a flaccid vesicle was aspirated to a prescribed, subcritical tension while being manipulated to a position between two platinum wire electrodes separated by ~1 mm. A 60 μsec square-shaped pulse was applied across the electrodes at intervals that varied from seconds to minutes depending on the postporation dynamics of the vesicle (see below). The applied potential was increased at discrete intervals until membrane rupture was observed. A typical electroporation event at low applied tension is shown in Fig. 3. The electrodes were arranged parallel to the pipette, generating an electric field $\mathbf{E}$ as illustrated, and the suction pressure was sufficient to hold the vesicle in the micropipette. A first image taken at zero applied field (0 msec) demonstrates the integrity of the membrane by showing a phase-dense vesicle interior (sucrose solution) against a phase-light exterior (equiosmolar glucose). Dramatic rupture within 1–2 video frames of the applied pulse was invariably indicated by a "jet" of released sucrose; such jets always occurred at focal point(s) on the membrane where the surface normal is parallel/antiparallel to $\mathbf{E}$. However, the dynamics of pore formation differed considerably from one membrane system to another. Membranes composed of OB16 (Fig. 3) typically showed *two* very large, antipodal pores that grew to many microns in size over seconds. Despite low tensions, pore growth continued and completely rendered the

TABLE II. Average values for the critical tension (at $V_m = 0$) and critical voltage (at $r \approx 0$). Fitted values for capacitance at rupture, associated surface charge and robustness R.

Molecule	τ_c (pN/nm)	V_c (V)	C_m (μF/cm^2)	σ_c (C/m^2)	R (V pN/nm)
SOPC	9	1.1	1.5	0.016	9.9
OE7	20	4.0	0.26	0.01	79.7
OB16	19	3.95	0.24	0.01	74.8
OB18	31	8.6	0.08	0.007	265.8

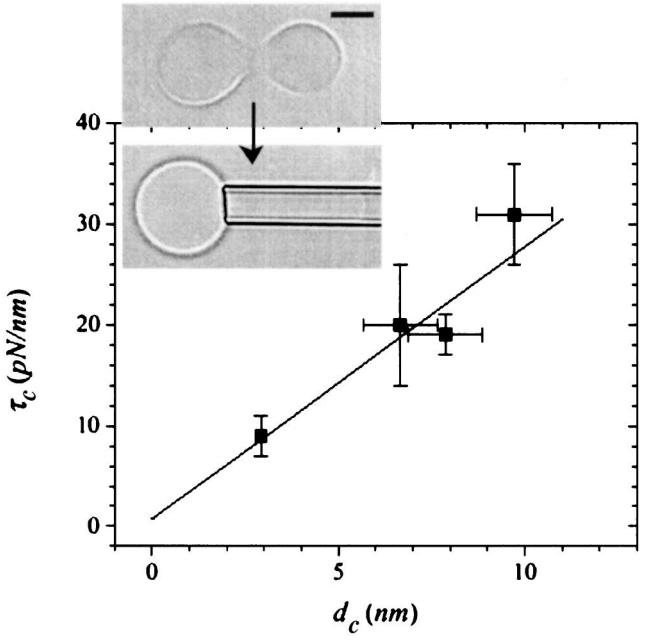

FIG. 2. The lysis tension τ_c at zero applied electric field is plotted as a function of the hydrophobic thickness d_c for (left to right) SOPC, OE7, OB16, and OB18 vesicles. Tension in the membrane is determined from the aspiration pressure ΔP by the application of the Laplace law to give $\tau = 0.5\Delta P R_v R_p/(R_v - R_p)$, where R_v is the external vesicle radius and R_p is the internal radius of the micropipette. Inset shows aspiration of a flaccid vesicle. Scale bar is 10 μm.

OB16 polymersomes. Phospholipid vesicles, in contrast, showed more rapid and even reversible pore dynamics at vanishing tension, as described by others [20–22]. Polymersomes of the smallest copolymer, OE7, exhibited liposomelike dynamics, whereas polymersomes composed of the largest copolymer, OB18, were far more protracted in their poration dynamics. With OB18, encapsulated sucrose was invariably lost over periods of *tens* of seconds, with weak, barely visible jets implying relatively small but sustained pores. Interestingly, Klotz *et al.* [22] have shown that macromolecules that bind strongly to lipid membranes increase both the capacitance and the inertia of the membrane—in agreement with our results for thicker membranes.

Kinetic diversity in membrane poration is understood at a first level in terms of the interplay between edge energy, characterized by a line tension λ that tends to close

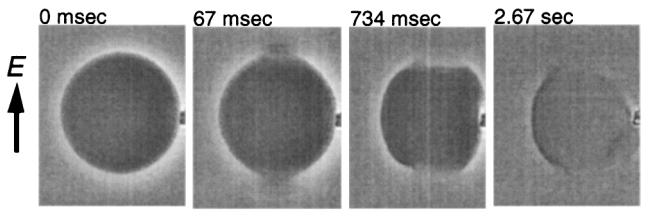

FIG. 3. Electrocompressive rupture of an OB16 polymersome with an initial diameter of ~40 μm. The holding tension is below 2 pN/nm, and the breakdown potential is ~4 V.

the pore, and the work done by any *dynamic* membrane tensions that tend to force the pore open [23]. A balance between these two energies gives the metastable pore size $r_0 = \lambda/\tau$, above which the pore will grow—provided sufficient tension is maintained [23]. Sandre *et al.* [21] recognized the important role of viscosities in vesicle pore dynamics. In the limit of vanishing tension, the rate of pore closure was postulated to scale as λ/η_s, where η_s is the surface viscosity. Although λ is expected—from simple bending energy considerations of a hydrophilic pore—to increase in linear proportion to d, separate measurements of the lateral diffusion of copolymers (Lee *et al.* [24]) suggest that η_s increases strongly with $\bar{M}_n$ and is at least tenfold greater in the present polymersomes compared to lipid membranes. Moreover, the $\bar{M}_n$ of both OB16 and OB18 exceed the relevant entanglement molecular weights (~2 to 3 kDa), so that the polymeric nature of the present systems provides a clear basis for the slowed pore dynamics.

The transmembrane potential V_m was calculated previously for a spherical shell [9] as $V_m = 1.5 R_v E \cos\theta[1 - \exp(-t/t_c)]$, where R_v is the radius of the vesicle and θ is the angle between the membrane surface normal and $\mathbf{E}$. The charging time t_c is given by $t_c = R_v C_m(\rho_i + 0.5\rho_e)$, where ρ_i and ρ_e are internal and external solution resistivities, respectively. In this work, t_c is orders of magnitude smaller than the pulse duration used. To assess coupling of the mechanical and electrical stresses as suggested by Eq. (1), polymersomes were aspirated to a set tension and subsequently subjected to electrical stresses as explained above. At each imposed tension, V_c was determined and the resulting points plotted in the $\tau - V_m$ plane (Fig. 4). The data show that the higher the membrane tension the lower the breakdown potential. For OB18, the results are remarkable: this ~15-nm-thick membrane can transiently withstand the potential of a 9 V battery.

Fitting the rupture data (τ, V_c) for each self-assembled membrane system by Eq. (1) readily generates an amphiphile-specific estimate of C_m at rupture (Table II). Within this phase space spanned by τ and V_m, the area under each parabolic segment provides a phenomenological measure of the range of electromechanical function or robustness. For SOPC, this robustness is very small (see Table II); for polymersomes, in contrast, the robustness can be orders of magnitude larger. Fitted values of polymersome C_m are nonetheless very low compared to those reported for lipid membranes, ~1 μF/cm^2 [9,22]. This is qualitatively consistent with the enhanced thickness of polymersome membranes since $C_m \approx \epsilon/d_c$, where ϵ is the hydrophobic dielectric constant. On the other hand, V_c at $\tau = 0$ increases considerably with d_c [see Eq. (1) and Fig. 4]. By definition, the surface charge at rupture $\sigma_c = C_m V_c$ should then be independent of d_c. Indeed, Table II indicates that σ_c varies by only a factor of about 2 within this structurally diverse set of membrane systems studied.

Polymersomes made from OB16 and OB18 offer the further possibility of cross-linking the membrane core.

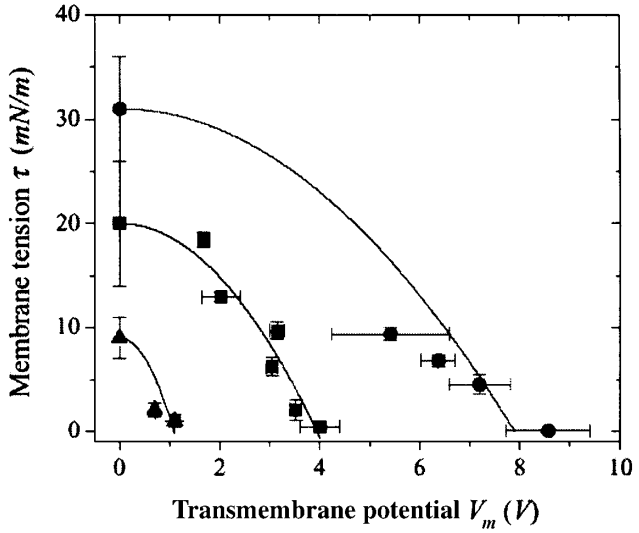

FIG. 4. Membrane tension τ versus transmembrane potential V_m. Rupture results are plotted for SOPC (triangles), OE7 (squares), and OB18 (circles). The solid lines correspond to parabolic fits using Eq. (1) in each case, giving the capacitance at rupture. The results for OB16 are omitted for clarity as they overlap with the results for OE7.

Free radical polymerization in solution [25] proves highly effective with dramatic increases in the robustness of the membranes. Simple osmotic rupture tests—where large vesicles are observed to burst after suspension in a sufficiently hypotonic solution—indicate that τ_c of cross-linked membranes are of order $\sim 10^3$ pN/nm. Thus $\Sigma_c \approx$ 1000 atm. Using such values in Eq. (1) and assuming values for C_m listed in Table II, V_c for the cross-linked OB's are estimated to exceed 125 V for 60 μsec pulses. The electromechanical stresses generated by the coupling of micropipette aspiration and electroporation techniques used here are insufficient to rupture these cross-linked polymersomes.

Electrically excitable cells, particularly neurons, control and propagate electrochemical potentials for signaling purposes [1], but the transmembrane voltages employed are always constrained by physical limits of a self-assembled lipid membrane system. The results here with a series of self-assembling biomimetic diblock copolymers considerably expand these limits, and clearly indicate the overall electromechanical robustness of hyperthick membranes. As might be expected, τ_c and V_c both increase with d, while C_m decreases and σ_c hardly changes. Although a microscopic theoretical treatment of membrane electroporation is lacking, the capacitance and insulation properties of such self-assemblies provide a more physically reliable basis for microelectronics applications such as sensor platforms and those that might exploit conducting copolymer segments. In addition, drug delivery applications could benefit through formulations of robust copolymer vesicles that reversibly reseal or not when challenged by sufficient membrane tensions and/or voltages.

H. A. E. and H. B. thank R. Parthasarathy for discussions and comments. H. A. E. was supported by an NIH/NHLBI T32HL-07954 training grant. D. E. D. gratefully acknowledges discussions with D. A. Hammer and E. A. Evans. Funding was provided by NSF-MRSEC at the University of Minnesota and University of Pennsylvania, and NASA.

[1] B. Alberts *et al., Essential Cell Biology* (Garland Publishing, New York, 1997).
[2] P. Fromherz and A. Stett, Phys. Rev. Lett. **75**, 1670 (1995); M. P. Maher *et al.,* J. Neurosci. Meth. **87**, 45 (1999).
[3] E. A. Evans *et al.,* Science **273**, 933 (1996); A. Karlsson *et al.,* Nature (London) **409**, 150 (2001).
[4] B. M. Discher *et al.,* Science **284**, 1143 (1999); B. M. Discher *et al.,* Curr. Opin. Colloid Interface Sci. **5**, 125 (2000).
[5] R. M. Hochmuth *et al.,* Biophys. J. **70**, 358 (1996).
[6] J. Dai and M. P. Sheetz, Biophys. J. **77**, 3363 (1999); E. Evans and A. Yeung, Biophys. J. **56**, 151 (1989).
[7] R. Simson *et al.,* Biophys. J. **74**, 514 (1998); H. Ra *et al.,* J. Cell Sci. **12**, 1425 (1999).
[8] G. Lippmann, Ann. Phys. **149**, 546 (1873).
[9] E. Neumann *et al., Electroporation and Electrofusion in Cell Biology* (Plenum, New York, 1989); D. C. Chang *et al., Guide to Electroporation and Electrofusion* (Academic, San Diego, 1992).
[10] J. C. Weaver, Radio Sci. **30**, 205 (1995).
[11] E. Neumann and S. Kakorin, Biophys. Chem. **85**, 249 (2000).
[12] D. V. Zhelev and D. Needham in *Biological Effects of Electric and Magnetic Fields,* edited by D. O. Carpenter and S. Ayrapetyan (Academic, San Diego, 1994).
[13] D. Needham and R. M. Hochmuth, Biophys. J. **55**, 1001 (1989).
[14] M. W. Matsen and M. Schick, Curr. Opin. Colloid Interface Sci. **1**, 329 (1996); D. A. Hajduk *et al.,* J. Phys. Chem. B **102**, 4269 (1998).
[15] M. A. Hillmyer and F. S. Bates, Macromolecules **29**, 6994 (1996).
[16] Y-Y. Won *et al.,* J. Phys. Chem. B **104**, 7134 (2000).
[17] H. Bermudez *et al.* (unpublished).
[18] K. Olbrich *et al.,* Biophys. J. **79**, 321 (2000); W. Rawicz *et al., ibid.* **79**, 328 (2000).
[19] F. R. Young, *Cavitation* (McGraw-Hill, New York, 1989).
[20] D. Zhelev and D. Needham, Biochim. Biophys. Acta **1147**, 89 (1993).
[21] O. Sandre *et al.,* Proc. Natl. Acad. Sci. U.S.A. **96**, 10 591 (1999).
[22] K-H. Klotz *et al.,* Biochim. Biophys. Acta **1147**, 161 (1993).
[23] M. Winterhalter and W. Helfrich, Phys. Rev. A **36**, 5874 (1987).
[24] J. C-M. Lee *et al.* (unpublished).
[25] Briefly, crosslinking was initiated by the water-soluble redox pair of potassium persulfate ($K_2S_2O_8$) and sodium metabisulfite ($Na_2S_2O_5$) ferrous sulfate ($FeSO_4 \cdot 7H_2O$). For more details see Y-Y. Won *et al.,* Science **283**, 960 (1999).